Agricultural and Forest Meteorology, 54 (1991) 107–136
Elsevier Science Publishers B.V., Amsterdam

Physiological and environmental regulation of stomatal conductance, photosynthesis and transpiration: a model that includes a laminar boundary layer*

G. James Collatz[a], J. Timothy Ball[b], Cyril Grivet[a] and Joseph A. Berry[a]
[a]*Carnegie Institution of Washington, Department of Plant Biology, 290 Panama Street, Stanford, CA 94305, USA*
[b]*Desert Research Institute, PO Box 60220, Reno, NV 89622, USA*

(Received 1 November 1989; revision accepted 22 October 1990)

ABSTRACT

Collatz, G.J., Ball, J.T., Grivet, C. and Berry, J.A., 1991. Physiological and environmental regulation of stomatal conductance, photosynthesis and transpiration: a model that includes a laminar boundary layer. Agric. For. Meteorol., 54: 107–136.

This paper presents a system of models for the simulation of gas and energy exchange of a leaf of a C_3 plant in free air. The physiological processes are simulated by sub-models that: (a) give net photosynthesis (A_n) as a function of environmental and leaf parameters and stomatal conductance (g_s); (b) give g_s as a function of the concentration of CO_2 and H_2O in air at the leaf surface and the current rate of photosynthesis of the leaf. An energy balance and mass transport sub-model is used to couple the physiological processes through a variable boundary layer to the ambient environment.

The models are based on theoretical and empirical analysis of g_s and A_n measured at the leaf level, and tests with intact attached leaves of soybeans show very good agreement between predicted and measured responses of g_s and A_n over a wide range of leaf temperatures (20–35°C), CO_2 concentrations (10–90 Pa), air to leaf water vapor deficits (0.5–3.7 kPa) and light intensities (100–2000 μmol $m^{-2} s^{-1}$).

The combined models were used to simulate the responses of latent heat flux (λE) and g_s for a soybean canopy for the course of an idealized summer day, using the 'big-leaf' approximation. Appropriate data are not yet available to provide a rigorous test of these simulations, but the response patterns are similar to field observations. These simulations show a pronounced midday depression of λE and g_s at low or high values of boundary-layer conductance. Deterioration of plant water relations during midday has often been invoked to explain this common natural phenomenon, but the present models do not consider this possibility. Analysis of the model indicates that the simulated midday depression is, in part, the result of positive feedback mediated by the boundary layer. For example, a change in g_s affects A_n and λE. As a consequence, the temperature, humidity and CO_2 concentration of the air in the proximity of the stomata (e.g. the air at the leaf surface) change and these, in turn, affect g_s. The simulations illustrate the possible significance of the boundary layer in mediating feedback loops which affect the regulation of stomatal conductance and λE. The simulations also examine

*This is Carnegie Institution of Washington, Department of Plant Biology publication no. 1074.

0168-1923/91/$03.50

the significance of changing the response properties of the photosynthetic component of the model by changing leaf protein content or the CO_2 concentration of the atmosphere.

INTRODUCTION

Transpiration and latent heat flux (λE) from vegetated surfaces are dependent on a number of interacting environmental and biological processes. One of the key elements of this system, the diffusive conductance of leaf surfaces to water vapor, may vary over a wide dynamic range and is controlled by physiological mechanisms. Most of the transpired water vapor, except when plant surfaces are wet, must pass through the stomata penetrating the leaf epidermis. It is generally accepted that these structures function to restrict water loss from the photosynthetic cells of the leaf mesophyll, yet they must also permit CO_2 to diffuse into the leaf to support photosynthesis. Complex physiological mechanisms adjust the opening of stomata in response to changes in environmental conditions, thus affecting the aggregate stomatal conductance of leaves (g_s) and the canopy. Stomatal conductance is sensitive to the intensity of short-wave radiation (R_s), humidity of the air (e_a), CO_2 partial pressure of the air (c_a), leaf temperature (T_l), drought stress and time of day, as well as to physiological conditions in the plant (Jarvis, 1976; Stewart, 1988; Jones and Higgs, 1989). Some aspects of the stomatal mechanism, e.g. the turgor-dependent movements that open or close the pore, are fairly well understood (see Raschke, 1979; MacRobbie, 1987), but the ion transport processes and the sensory system that control these are still a puzzle.

Models that attempt to predict stomatal conductance directly from factors of the environment, while making no attempt to address the fundamental underlying mechanisms, are presently the approach of choice in constructing models of transpiration and energy balance of land surface. Of the models available, some have been obtained by correlation analysis of estimates of canopy conductance (estimated by inversion of the Penman–Monteith equation) with certain environmental variables such as solar radiation and humidity (Lindroth and Halldin, 1986; Stewart, 1988). Other models are based on direct studies of the stomatal conductance of leaves, either in controlled or natural environments (Jarvis, 1976; Avissar et al., 1985; Jones and Higgs, 1989). Some canopy models (Choudury and Monteith, 1986; Stewart, 1988; Gash et al., 1989) and global models (Sato et al., 1989) have included stomatal response functions. These studies have shown that physiologically mediated feedbacks affecting stomatal conductance may have strong influences on surface energy balance, and indicate the importance of having accurate models of this key process.

A general problem with correlative models of the type presently in use is that these tend to be specific to particular vegetation–climate systems (e.g.

Gash et al., 1989; Jones and Higgs, 1989). Parameters, such as the maximum stomatal conductance, or the sensitivity of g_s to the air to leaf vapor pressure deficit, must be readjusted (by empirical correlation) to fit a particular vegetation type or prevailing condition. A truly mechanistic model might be expected to provide a more general basis to predict stomatal responses, but such a model is not currently plausible.

In this paper, we will draw upon considerable body of work that has addressed the role of stomatal conductance in regulating the balance between transpiration and net uptake of CO_2 in photosynthesis. This work considers functional and theoretical constraints that have presumably been major factors in the evolution of the regulatory mechanisms of stomata and, in our opinion more general and realistic models of g_s can be developed from proper consideration of these constraints. Nevertheless, the model we present is still largely empirical. Some parts of it, particularly those dealing with photosynthetic CO_2 uptake, are based on fundamental properties of the biochemical mechanisms.

The theoretical treatment begins with the premise that stomata serve the conflicting roles of permitting CO_2 to diffuse into the leaf to support photosynthesis and restricting the diffusion of water vapor out of the leaf. To succeed fully in one role must necessarily lead to total failure in the other role, and it has been argued that the regulatory system must strike an appropriate compromise between permitting photosynthesis and restricting water loss (Cowan, 1977; Raschke, 1979). Cowan and Farquhar (1977) proposed that the regulation of g_s over an interval of time would be optimal if no other response trajectory could have led to a smaller total water loss for a given carbon gain (or a larger carbon gain for a given water loss) integrated over that interval of time. They present a mathematical solution to this problem and hypothesize that the mechanisms that regulate stomata should approach, through natural selection, this theoretical optimum. There is a great deal of experimental work that lends support to this theory (for a review, see Farquhar and Sharkey, 1982).

The model presented here developed from attempts to apply the Cowan–Farquhar theory at the level of the leaf in order to understand the regulatory responses of stomata to specific factors of the environment. The theory requires that we consider the responses of both photosynthesis and transpiration in such an analysis. Work by Wong et al. (1979) and Ball and Berry (1982) led to the concept that the responses of stomata to changes in the environment can be partitioned into components that are dependent on photosynthesis and others that are independent of photosynthesis. For example, a change in light (which primarily affects the kinetics of photosynthesis), with all other factors held constant, generally causes g_s to respond so as to maintain a constant proportionality of g_s to A_n. On the other hand, a change that affects only the kinetics of water vapor diffusion (e.g. a change in the diffusion gra-

dient, $\mathscr{D}$) generally causes the g_s/A_n ratio to change. The analysis of Ball (1988), which provides the basis for the model used here, includes an implicit dependence of g_s on photosynthesis. A_n was measured together with other relevant environmental parameters and included as an independent variable in analysing the responses of g_s. Most of the remaining variation in g_s could be attributed to effects of the CO_2 and H_2O concentration of the air in the local environment of the stomata. In the system of models described here, we make use of a photosynthesis model based on the work of Farquhar et al. (1980) to obtain A_n as a function of environmental variables.

A significant feature of the present stomatal model is that it is structured to consider the influence of the laminar boundary layer (which affects the local environment of the stomata) on the regulatory responses of the leaf system. The leaf surface is considered as the boundary separating the physiological processes that operate within the leaf from the transport processes that operate in the boundary layer (see Fig. 1), and the physiological model was parameterized with reference to environmental conditions specified at the leaf surface (see Ball, 1987). It is important to note that this does not necessarily imply that the regulatory mechanisms of the stomata 'sense' the concentrations at the leaf surface. Rather, the use of surface conditions is a logical requirement for separating the transport of sensible heat, CO_2 and H_2O through a laminar boundary layer of variable conductance and the physiological processes of the leaf.

The physiological models (for A_n and g_s) are combined with a model giving the environment at the leaf surface and the leaf energy balance as a function

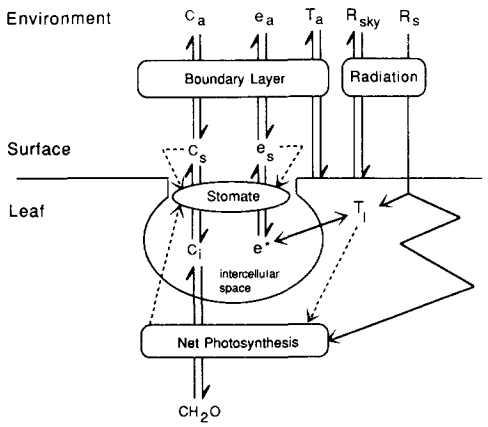

Fig. 1. A scheme showing the mass and energy fluxes along with the interactions between these considered in the complete model. Fluxes are shown as solid lines. Regulatory interactions are shown as dashed lines. *c*, *e* and *T* stand for CO_2, H_2O vapor concentrations and temperature, respectively. The subscripts a, s and l, refer to properties in ambient air, at the leaf surface and of the leaf, respectively. R_{sky} specifies the long-wave length radiation input from the sky and R_{solar} represents solar radiation.

of g_s. These interacting models are solved by a numerical method, and we present simulations of the responses of g_s and latent heat flux (λE) of a soybean leaf in free air with the boundary layer treated as an independent variable.

The simulations illustrate the possible significance of the boundary layer in mediating feedback loops which affect the regulation of stomatal conductance and λE. The simulations also examine the significance of changing the response properties of the photosynthetic component of the model by changing leaf protein content or the CO_2 concentration of the atmosphere.

MODEL DESCRIPTION

Below we describe the models used and briefly discuss their parameterization. A general scheme showing the structures, processes, fluxes and regulatory interaction considered here is presented in Fig. 1. An Appendix to this article provides definition of terms, parameter values and equations used in our simulations of this system.

Stomatal sub-model

Ball (1988) and Ball and Berry (1991) proposed an equation to describe the response of g_s to the rate of net CO_2 uptake (A_n) and the relative humidity (h_s) and CO_2 mole fraction (c_s) of the air at the leaf surface

$$g_s = m\frac{A_n h_s}{c_s} + b \qquad (1)$$

The terms m and b are, respectively, the slope and intercept obtained by linear regression analysis of data from gas exchange studies with single leaves in a ventilated, temperature-controlled cuvette. Surface concentrations are functions of ambient concentrations, leaf boundary-layer conductance (g_b) and g_s. These are routinely evaluated in gas exchange studies, as described by Ball (1987). In this paper, we will follow the convention of units introduced by Cowan (1977) and in common use in the physiological literature. Conductances are specified in units of mol m^{-2} s^{-1} and the diffusion gradients are given in mole fraction (i.e. mol mol^{-1}). For convenience, a conductance of 1 cm s^{-1} is approximately 0.4 mol m^{-2} s^{-1} at 25°C and an atmospheric pressure $P = 101.3$ kPa. The flux of CO_2 uptake, A_n, is in units of μmol m^{-2} s^{-1}, c_s is in μmol mol^{-1}, h_s is a unitless ratio, m is unitless and b is in conductance units.

Equation (1) was developed from a series of gas exchange studies described in detail by Ball and Berry (1991). Briefly, these studies were structured to examine the dependence of g_s on each of the independent variables A_n, c_s and h_s. Since it was not practical to always arrange conditions to keep A_n constant while other variables were changed, a sequential analysis protocol

was adopted. First, building on the work of Wong and others (Wong et al., 1978, 1979, 1985a,b,c), it was established that g_s varies in proportion to A_n when c_s and h_s were held constant. This permitted A_n to be brought to the left side of the equation (e.g. eqn. (1)), so that the effect of h_s and c_s could be examined against g_s/A_n as the dependent variable. Second, it was observed that the value of the proportionality constant varied according to consistent patterns when either c_s or h_s was changed: (a) g_s/A_n varied in proportion to $1/c_s$ provided h_s was held constant; (b) g_s/A_n varied in direct proportion to h_s with c_s constant. Finally, it was established that the variables appeared to interact multiplicatively over physiologically interesting ranges of values.

The use of h_s, as opposed to the actual vapor pressure gradient ($\mathscr{D}_s$), was decided from a series of experiments which examined the response to $\mathscr{D}_s$ at different temperatures. Studies of Ball and Berry (1982, 1991) indicated that the sensitivity of g_s/A_n to $\mathscr{D}_s$ decreased with increasing temperature (see Fig. 5), and they found that this could be approximated as $g_s/A_n \propto (1-\mathscr{D}_s/e^*)$ where e^* is the saturation vapor pressure of water at T_l. The term $(1-\mathscr{D}_s/e^*)$ can be simplified to relative humidity, h_s. At the present time, we view the use of h_s in eqn. (1) as a mathematical 'convenience'. There is no direct evidence for a humidity sensor. In fact, recent studies by Mott and Parkhurst (1991) indicate that the response of g_s at any constant temperature is probably controlled by the rate of transpiration, but they also observed that the sensitivity of g_s changed with temperature approximately as described by eqn. (1).

Norman and Polley (1989) and Ball and Berry (1991) reported regression parameters for several C_3 and C_4 species. The parameters of eqn. (1), i.e. the slope factor m and intercept b, may be determined from a linear regression of g_s as a function of the product $A_n h_s/c_s$, where these terms are obtained from measurements of leaf gas exchange conducted with intact attached leaves under controlled conditions. To be assured that the regression is appropriately weighted, the data should include a range of CO_2 concentrations, light intensities, temperatures and atmospheric humidities that span the range of interest. Ball and Berry (1991) caution that eqn. (1) should not be used when $A_n \to 0$ (at $Q_p < 50$ μmol m^{-2} s^{-1} or $c_s < 100$ μmol mol^{-1}), and data in these ranges should not be included in the linear regression analysis. Leuning (1990) found that using $c_s - \Gamma$, where Γ is the CO_2 compensation concentration, gave a better fit at low values of c_s.

Photosynthesis sub-model

Prediction of g_s according to eqn. (1) requires that A_n be known. A_n is a useful quantity to know since it is directly related to the primary productivity of leaves and canopies, but its relevance in this discussion is limited to the dependence of g_s on A_n.

The CO_2, light and temperature dependence of A_n (following Farquhar et al. (1980) and Kirchbaum and Farquhar (1984)) is estimated as

$$A_n \approx \min\begin{Bmatrix} J_E, f(Q_p, a, p_i, T_l) \\ J_C, f(V_m, p_i T_l) \\ J_S, f(T_l, V_m) \end{Bmatrix} - R_d, f(T_l, V_m) \quad (2)$$

where the terms J_E, J_C and J_S are separate rate expressions for photosynthetic CO_2 uptake in terms of a different rate-limiting step in the overall process of photosynthesis (J_E, light; J_C, ribulose bisphosphate (RuBP) carboxylase (or Rubisco); J_S, sucrose synthesis), and R_d is the rate of 'day' respiration. The actual rate approaches the minimum (or most limiting) rate. In practice, the first term on the right in eqn. (2) is transformed to a continuous function with a smooth transition from one limiting factor to another using nested quadratic equations. These and the expressions for J_E, J_C and J_S are given in the Appendix. The latter are functions of kinetic constants, leaf properties (i.e. the catalytic capacity, V_m, of the CO_2-fixing enzyme, Rubisco, and the absorptance to Q_p, a) and environmental parameters (i.e. the leaf temperature, T_l, the incident flux of photosynthetically active photons, Q_p, and the partial pressure of CO_2 in the intercellular air spaces of the leaf, p_i). Note that $p_i = c_i \times P$, where c_i is in mole fraction and P is the atmospheric pressure.

A complete listing of the kinetic parameters, their temperature dependencies and the equations used in the model is presented in the Appendix. The parameters that may vary from leaf to leaf are the absorptance to Q_p, a (generally, $a \sim 0.9$), and the maximum capacity of the carboxylase reaction (V_m).

Selection of the appropriate value to use for the V_m of Rubisco is the major problem in parameterizing the photosynthesis model. For the simulations reported here, we estimated this by an in vivo assay. Gas exchange studies are used to measure the slope of the response of A_n to p_i (dA_n/dp_i) at light saturation, at a known leaf temperature (about 25 °C) and at $p_i = \Gamma_*$. V_m may then be calculated according to eqn. (A6), as described in the Appendix. It is also possible in some cases to measure V_m directly by extracting leaf proteins and assaying the enzyme activity (see Woodrow and Berry, 1988). With appropriate calibration experiments, it is possible to estimate V_m from measurements of total leaf nitrogen since Rubisco is a significant and fairly constant fraction of total leaf protein (see Evans and Seemann, 1989).

Combining the sub-models

These two sub-models may be viewed as being interdependent at the leaf level. The photosynthesis model requires p_i as an input variable, and this is a function of c_s and g_s. The latter can be obtained from the stomatal model, but this requires a value of A_n. A simultaneous solution can be obtained by numerical methods.

Tests of the models

Figure 2 shows a plot of g_s predicted from eqn. (1) compared with measured values of g_s obtained in 169 separate gas exchange measurements with several different leaves (see Ball (1987) and Ball and Berry (1991) for experimental details). These measurements were conducted under a wide variety of conditions (T_l=20–35°C, Q_p=100–2000 μmol m^{-2} s^{-1}, h_s=0.45–0.90, c_s=100–900 μmol mol^{-1}). The high correlation between predicted and measured g_s (r^2=0.92) illustrates the predictive power of this sub-model. The values of the slope factor m and intercept b were determined from an analysis of an independent set of measurements (Ball and Berry, 1990).

Figure 3 shows a plot of predicted vs. measured values of A_n from gas exchange studies of leaves of *Glycine max*. Predicted A_n was calculated from the photosynthesis sub-model using measured values of p_i, Q_p, and T_l obtained at same time as the measurement of A_n. The value for V_m was estimated as described in the Appendix. Three groups of leaves from different growth regimes and having different V_m values were included in this study. The set of measurements is identical to those included in Fig. 2. The analysis shows a very good correspondence (r^2=0.93) between the predicted and the measured values of A_n.

Figure 4 shows a plot of the predicted value for g_s obtained by solving the combined sub-models compared with the actual measured values. The correlation (r^2=0.90) for the combined models provides strong empirical support for this approach to modeling g_s. A similar but independent test of a com-

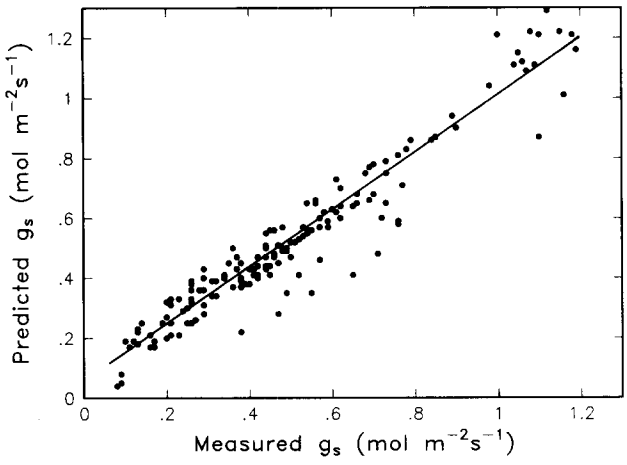

Fig. 2. Stomatal conductances measured in a leaf gas exchange cuvette, compared with those predicted by eqn. (1) using measured values of h_s, c_s and A_n. The line drawn through the points is a linear regression of data (y=0.95x+0.05, n=169, r^2=0.92).

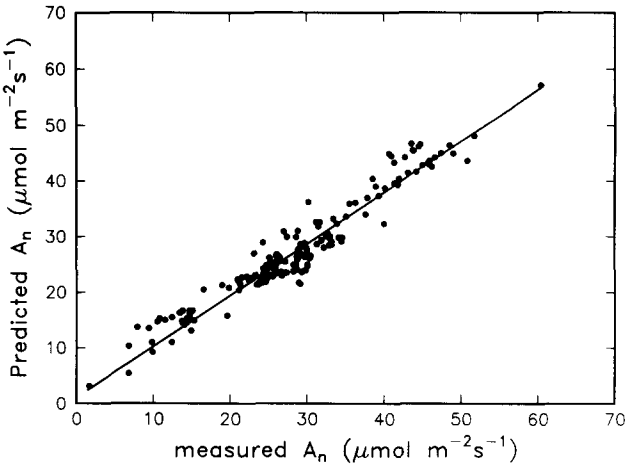

Fig. 3. Net photosynthetic rates measured in a leaf gas exchange cuvette compared with those predicted by the photosynthesis model. Measured values for c_i, Q_p, V_m and T_l were used as inputs of the model. The line represents a linear regression of the data ($y=0.9x+1.89$, $r^2=0.93$).

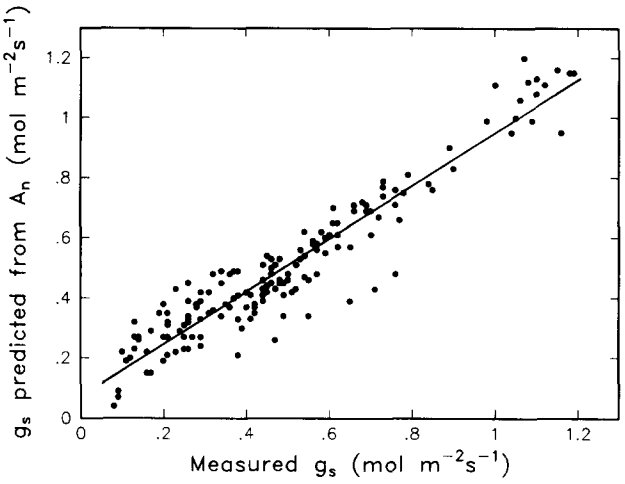

Fig. 4. Measured stomatal conductances compared with those predicted by the combined sub-models for net photosynthesis and stomatal conductance. Input parameters were h_s, c_s, Q_p, V_m and T_l. The line is drawn from a linear regression of the data ($y=0.87+0.07$, $r^2=0.90$).

bined photosynthesis model with the Ball and Berry stomatal model is presented by Leuning (1990).

Comparison with other stomatal models

The combination of the two sub-models (eqns. (1) and (2)) provides g_s

as a function of environmental variables, using prediction of A_n as an intermediate step. If A_n is not of interest (only g_s), then we may regard the above model as essentially equivalent to other empirical models that give g_s directly as a function of environmental variables. Here, we will examine some of the similarities and differences that distinguish this model from other models.

First, as noted in the introduction, the Ball–Berry model is parameterized to be driven by the environmental conditions at the leaf surface, while other models (Jarvis, 1976; Avissar et al., 1985; Lindroth and Halldin, 1986) relate stomatal response to ambient conditions. It seems reasonable to assume that stomata respond to their local environment and to expect that this local environment should be influenced by the boundary layer of the leaf or canopy, and by the fluxes of heat, H_2O and CO_2 at the leaf surface (Choudhury and Monteith, 1986). The Ball–Berry model is, thus, the only model structured to permit realistic treatment of these influences of g_b on the regulatory responses of stomata. There is no intrinsic reason, however, preventing other models from being parameterized to the surface environment.

Avissar and Mahrer (see Avissar et al., 1985) proposed a model that describes the attenuation of stomatal conductance from some maximum value by vapor pressure deficit of the air ($\mathscr{D}_a$), ambient partial pressure of CO_2, p_a, T_l and total radiation (R_t) using a threshold-type function. This form predicts that stomata tend to go from being fully open to completely closed over a narrow range of an environmental variable. We observe, however, that stomata generally respond continuously over a broader range of variable values. The Ball and Berry (1991; B–B), Jarvis (1976, J) and Lohammer (Lindroth and Halldin, 1986; L) models show more gradual responses to variables and only these latter models will be discussed in detail, keeping in mind that the Avissar–Mahrer model will agree with the others as g_s approaches its maximum or minimum values.

Both the L and J models describe g_s as a function of a maximum stomatal conductance (g_{max}) by scaling this value with a series of factors (each between 0 and 1) which are functions of environmental variables taken separately (e.g. temperature, R_t, $\mathscr{D}_a$). The B–B model includes direct stomatal responses to CO_2 and humidity, plus indirect responses to light, CO_2 and temperature, through the effects of these variables on A_n. The model for A_n is structured such that strong interactions may occur between temperature, light and CO_2, while the L and J models differ in assuming that these factors act independently and are multiplicative. We will return to this point later. To begin our comparison, we note that the models are structurally similar in their treatment of the response of g_s to atmospheric humidity, and all three models can be written in the form

$$g_s = g'_s \times f(\mathscr{D}) + b \tag{3}$$

where g'_s is essentially the stomatal conductance under the conditions in ques-

tion in the absence of atmospheric drought, b is an intercept and $f(\mathscr{D})$ is the $\mathscr{D}$ response factor. For the B–B model, this factor is

$$f(\mathscr{D}) = h_s = 1 - \frac{\mathscr{D}_s}{e^*} \tag{4}$$

while for the J model

$$f(\mathscr{D}) = (1 - m' \mathscr{D}_a) \tag{5}$$

and the L model uses

$$f(\mathscr{D}) = \frac{1}{1 + m'' \mathscr{D}_a} \tag{6}$$

To appreciate the differences in these response functions, consider that a change in $\mathscr{D}$ may be driven by changes in ambient vapor pressure (e_a) or by a change in T_l which affects e^*, since $\mathscr{D} = e^* - e_a$. For the purpose of comparison, we will dispense with the distinction between $\mathscr{D}_a$ and $\mathscr{D}_s$ by assuming that g_b is large so that $T_l \rightarrow T_a$ and $\mathscr{D}_s \rightarrow \mathscr{D}_a$. Figure 5 compares the responses of g_s of a soybean leaf to a $\mathscr{D}$ imposed by varying e_a at constant temperatures of 20 or 35°C, and by varying temperature (20–37°C) at constant e_a. At any constant temperature, g_s decreases linearly with increasing $\mathscr{D}$. This is consistent with the form of the J model (eqn. (5)), but as shown (Fig. 5), the slope of the response of g_s to an imposed $\mathscr{D}$ (the value of m') is lower at 35°C than at 20°C. When $\mathscr{D}$ is increased by increasing temperature at constant e_a, g_s decreases hyperbolically (Fig. 5). This cannot be fit by a single value of m' (eqn. (5)). The empirical equation used in the L model (eqn. (6)) yields a

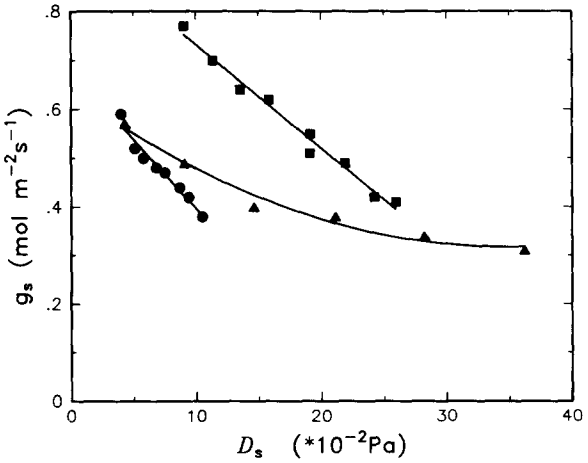

Fig. 5. The response of stomatal conductance to vapor pressure deficit imposed by changing the ambient or saturation vapor pressures; variable e_a at 20°C, (●); variable e_a at 35°C, (■); constant e_a at 20–37°C, (▲).

hyperbolic decrease in g_s with increasing $\mathscr{D}$. This approximates the response pattern observed with a temperature imposed $\mathscr{D}$, but it does not fit the constant temperature case. The curve shape of the L model may be related to the fact that it was developed from analysis of responses in a natural system (a forest canopy) where temperature was the major factor causing the $\mathscr{D}_a$ to vary. The B–B model fits both types of curve shown in Fig. 5 ($r^2=0.76$ for all data points). This is directly related to the presence of a temperature-dependent term (e^*) in the $\mathscr{D}$ response in the B–B model (eqn. (4)).

We now turn to the equations used to predict the value of g'_s of eqn. (3). This can include the response to a number of separate environmental variables. Using the terms of Jarvis (1976), this may be written as

$$g'_s = g_{max} \times h(\boldsymbol{Q}_p) \times i(T_l) \times j(c_a) \ldots \quad (7)$$

where the terms $h,i,j,\ldots$ are factors between 0 and 1. The L model uses a similar approach, but does not include a response to c_a or T. From eqns. (1) and (3), we may obtain for the present model

$$g'_s = \frac{m\boldsymbol{A}_n}{c_s} + \frac{b}{f(\mathscr{D})} \quad (8)$$

It should be noted that the appropriate value of $\boldsymbol{A}_n$ is that evaluated at the steady-state conditions (T_l, $\boldsymbol{Q}_p$, p_i) in question, and the value of $\boldsymbol{A}_n$ will vary with $\mathscr{D}$ to the extent that the values of T_l or p_i change with g_s. Thus, we still require a solution to the combined photosynthesis and stomatal sub-models to evaluate g'_s.

The term g_{max} of eqn. (7) is a hypothetical 'maximum stomatal conductance' that reflects intrinsic differences between leaves in stomatal density and size. In the present model, this parameter can be viewed as being directly related to the parameters that affect the maximum photosynthetic capacity of leaves, mostly the V_m activity of Rubisco, which is in turn related to the quantity of protein committed to photosynthetic functions. Thus, leaf-to-leaf variation in g_{max} may be highly correlated with leaf protein.

The environmental response factors to $\boldsymbol{Q}_p$, T and c_a of eqn. (7) are implicitly included in the $\boldsymbol{A}_n$ term of eqn. (8) and, as noted earlier, the photosynthesis model predicts a high degree of interaction between these factors. For instance, the response of $\boldsymbol{A}_n$ to temperature is such that the shape of the response curve and the apparent temperature optimum changes with the level of $\boldsymbol{Q}_p$ and the value of p_i. On the other hand, the J model uses a response function that yields a more or less symmetrical response, falling as temperature is increased or decreased from the optimum temperature. This function can be made to approximate the shape and temperature optimum of the photosynthesis model under any particular values of p_i and $\boldsymbol{Q}_p$, but the parameters of the curve would need to be changed if the environment changed. Similarly, the response of $\boldsymbol{A}_n$ to $\boldsymbol{Q}_p$ yields a curve that can be approximated by the

rectangular hyperbola used in the J and L models, but the parameters of this rectangular hyperbola would need to be changed if the temperature or p_i were changed. The interacting effects of temperature, Q_p and p_i on A_n are accurately depicted by photosynthesis model (see Fig. 3; Farquhar et al., 1980; Kirschbaum and Farquhar, 1984). Ball and Berry (1991) showed that responses of g_s are strongly correlated with A_n, and the data presented in Fig. 4 confirm that the approach taken here provides a good basis to predict g_s over a wide range of temperature, Q_p and p_i. It is also significant that the present model requires fewer adjustable parameters than the L or the J models.

Energy and mass balance sub-models

The model developed above requires knowledge of the value of several environmental parameters at the leaf surface. Under natural conditions, these are determined by the aerodynamic properties of the leaf, the wind speed, the fluxes of radiation and heat and gases exchanged between the leaf and its surroundings. Well-established equations for energy balance and mass transport can be used to describe this system as a function of g_s, g_b and the ambient environment (see Appendix). When the three models are combined, λE of a leaf or simple ('big-leaf') canopy can be calculated from environmental conditions (c_a, e_a, R_t, T_a and g_b) and the physiological characteristics of the surface (V_m, m and a).

There is a strong interaction between the sub-models of this system and a computer program was constructed to obtain a numerical solution. Using an initial guess for g_s (i.e. $g_s = 1$ mol m^{-2} s^{-1}) and p_i (i.e. $p_i = 15$ Pa) the program obtains T_l, A_n, g_s and p_i by iteration, using the Newton–Raphson method, until p_i is stable. (A copy of the program can be obtained from the authors on request.)

RESULTS OF SIMULATIONS

The simulations we are about to describe depict the responses of a single-sided, horizontal leaf in free air. However, we will discuss these results in terms of canopy responses, making the assumption that canopy processes can be approximated as a 'big leaf'. We acknowledge that this is not strictly valid since we do not treat structural features or the heterogeneous environment of a real canopy. We are encouraged in making this simplification by Raupach and Finnigan (1989), who defend the position that, "single-layer models of evaporation from plant canopies are incorrect but useful, whereas multilayer models are correct but useless". We adopt their pragmatic approach here (but we acknowledge that more realistic models may yield different results).

Our goal in these simulations is to examine the interaction of the boundary layer with the regulatory properties of stomata in natural systems. Previous

treatments of the influence of the conductances of the boundary layer and the stomata on evapotranspiration of plant surfaces (Jarvis and McNaughton, 1986) treat g_s as a prescribed variable (set at a constant plausible value), while boundary-layer conductance is permitted to vary. In reality, the value of g_b has an influence over the environmental conditions at the leaf surface, and these in turn affect and are affected by g_s. Our model permits g_s to be treated as a dependent variable when g_b is varied.

We have chosen to present simulations of λE and g_s over the course of a day rather than more abstract simulations where only boundary layer (for example) is varied. Our rationale is that this permits comparison to actual measurements of canopy or leaf fluxes which are generally reported as diurnal curves. Furthermore, many analyses of the dependence of canopy processes on environmental variables are extracted from analysis of such curves. Our simulations provide a basis to consider the significance of apparent responses of the system, given the fact that parameters such as R_s, T_a, $\mathcal{D}_a$ and g_b may covary over the course of a typical day.

Figure 6 shows the daily cycle of R_s, T_a and $\mathcal{D}_a$ used in our simulations. This is an idealized day, designed to represent typical summer conditions in temperate North American agricultural regions. Peak values for R_s, T_a and $\mathcal{D}_a$ are 900 W m^{-2}, 32°C and 3.5 kPa, respectively. During the day, R_s advances and declines symmetrically around noon; air temperature follows R_s, but lags by about 2 h; $\mathcal{D}_a$ tracks the march of T_a since e_a remains essentially constant.

Simulated responses of λE, g_s and A_n to the daily march of environmental conditions (Fig. 6) at different imposed values of g_b (0.3, 2 and 8 mol m^{-2} s^{-1}) are shown in Fig. 7. The maximum exchange of λE (Fig. 7(a)) occurs at the intermediate value of boundary-layer conductance (2 mol m^{-2} s^{-1} – a

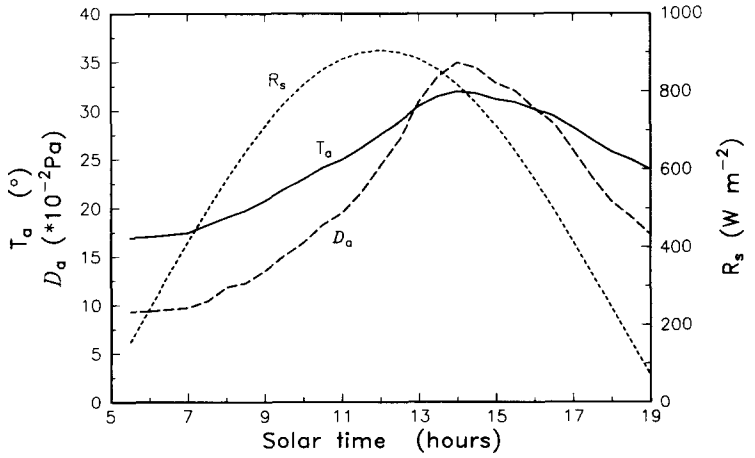

Fig. 6. The day courses of the environmental variables used in the simulations of latent heat flux and stomatal conductance.

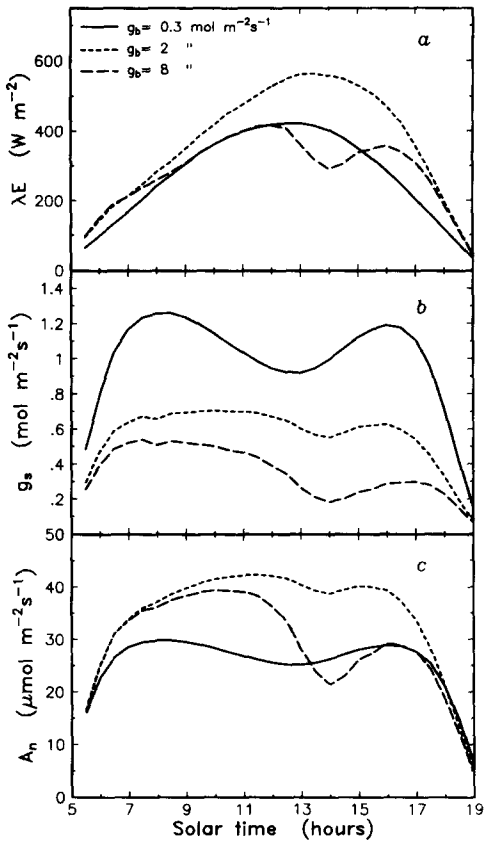

Fig. 7. Latent heat flux (a), stomatal conductance (b) and net photosynthesis (c) of a soybean canopy over the course of the day (Fig. 6) simulated at three values of boundary-layer conductances.

resistance of 20 s m^{-1}). This value is approximately that expected for a well-developed crop canopy with moderate winds. Decreasing or increasing the boundary-layer conductance, as might occur with changes in wind speed, results in a substantial attenuation of λE. The flux rises and falls with the changes in R_s and $\mathscr{D}_a$, except that a distinct midday depression is evident when the boundary layer is thin ($g_b = 8$ mol m^{-2} s^{-1}). This is associated with midday stomatal closure (Fig. 7(b)) and a midday depression of photosynthesis (Fig. 7(c)). The depressions in g_s and A_n are not as strongly expressed in λE at the lower values of g_b. This indicates that λE is not likely to be a good indicator of physiological responses in closed canopies (Raupach and Finnigan, 1989).

Midday depressions of g_s affecting A_n, and occasionally λE, have been observed in leaves (Beyschlag et al., 1986) and open natural canopies (Tan and Black, 1976; Cambell, 1989). The physiological models used in these simulations do not include any direct effect of the rate of transpiration or water

potential on photosynthesis. Such effects have often been invoked to explain the midday depression of λE observed in the field. We cannot exclude the participation of such effects, but the present analysis shows that it is not necessary to postulate these responses to obtain midday stomatal closure.

The simulations show a strong interaction between the imposed value of g_b and the value of g_s selected by the regulatory properties of the model (leaf). In general, g_s increases as g_b is decreased (Fig. 7(b)). This response tends to resist changes in (stabilizes) the total conductance. The humidity response of the stomatal mechanism is primarily responsible for this effect. The humidity of the air at the leaf surface tends to increase as g_b is decreased because more of the transpired water vapor is retained by the boundary layer. Referring to eqn. (1), this should cause g_s to increase. This response has the characteristics of a 'feedforward' response (Farquhar, 1978) since λE decreases substantially in going from 2 to 8 mol m^{-2} s^{-1}, while the evaporative demand imposed by the environment increases. It is interesting that the water-use efficiency ($A_n/\lambda E$) is very similar at $g_b=2$ and 8 mol m^{-2} s^{-1}, despite the higher evaporative demand at the higher value of g_b (compare Fig. 7(b) and 7(c)). Water-use efficiency is lowest at the low value of g_b, apparently because A_n is depressed.

The response of net photosynthesis is also of interest because it has a direct influence on stomatal conductance (see eqn. (1)). The strong depression of A_n during midday at $g_b=8$ mol m^{-2} s^{-1} (Fig. 7(c)) is driven by stomatal closure and depletion of intercellular CO_2. As noted, the closure of stomata may be initiated by the drying of the air at the leaf surface, but the decrease in A_n should have a positive feedback effect on g_s. The decrease in g_s caused by humidity leads to a decrease in A_n, that causes a further decrease in g_s.

The midday depressions of photosynthesis and g_s at low g_b (0.3 mol m^{-2} s^{-1}), are related by a different chain of cause and effect. The primary event leading to a decrease in g_s appears to be a decrease in A_n related to an increase in T_l, as the exchange of sensible and latent heat is restricted at low boundary-layer conductance. (Under these conditions, T_l is greater than the temperature optimum for photosynthesis.) According to eqn. (1), inhibition of A_n would lead directly to a depression of g_s. It should be noted however, that a decrease in g_s may also be expected to elicit a positive feedback on itself, mediated by the humidity response (humidity at the leaf surface would decrease if λE decreases and if T_l increases).

Figure 8 shows a plot of the leaf to air temperature difference as a function of $\mathscr{D}_a$ taken from a simulation of a daily curve at $g_b=2$ mol m^{-2} s^{-1}. This type of plot has been widely used as an indicator of water stress in crop canopies (Idso et al., 1981) and, more recently, as a basis for estimating aerodynamic and crop resistances (O'Toole and Real, 1986). The approximately linear decrease in T_l-T_a occurs over the interval of 09:00–15:00 h and the slope is -1.9°C kPa^{-1}. The pattern of response and the value of the slope is similar

to field observations made on several crop canopies (see O'Toole and Real, 1986). Analysis of these data using the approach of O'Toole and Real (1986) gives the mean values of $g_b = 2.3$ and $g_s = 0.6$ mol m^{-2} s^{-1}, while the actual values were somewhat different (see Fig. 7(b)). Faver and O'Toole (1989) have also noted that estimates of g_b from aerodynamic considerations are lower than those derived from analysis of plots similar to Fig. 8. In our simulations, g_s is not constant (see Fig. 7(b)), as their analysis assumes. Idso (1987) has used the existence of a linear response of $T_l - T_a$ to $\mathscr{D}_a$ (similar to Fig. 8) to argue that the conductance of crop canopies does not respond to humidity. The model used here includes a humidity response of g_s. Our simulations show that the linear response is not inconsistent with humidity control of g_s. tests of the accuracy of these simulations await more complete quantitative measurements of canopy fluxes and energy balance from systems that have been physiologically characterized.

In Fig. 7, g_b is treated as an independent variable that is held constant over the course of the day, when in reality g_b is dependent on other system variables and may change (over seconds or hours with changes in ventilation, and seasonally with changes in canopy structure). By plotting g_b and time as independent variables in three dimensions, we see a more complete picture of the dependence of λE on g_b (Fig. 9). In these simulations, we choose a range of g_b (0.1–10 mol m^{-2} s^{-1}) wider than is likely to occur in any natural canopy subject to high irradiance. The extremes may be approached by small leaves of open well-ventilated systems (e.g. a desert shrub) or by the large leaves of certain shade species (e.g. a banana tree) (see Grace, 1983), and

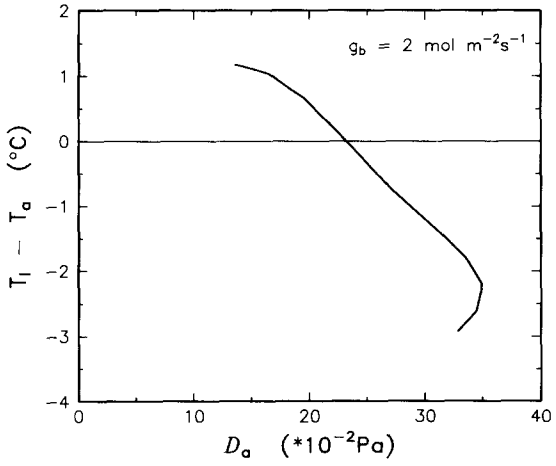

Fig. 8. The leaf temperature – air temperature difference plotted against the vapor pressure deficit of the air. Data taken from 09:00 to 15:00 h of a simulated day curve (Fig. 7) at $g_b = 2$ mol m^{-2} s^{-1}.

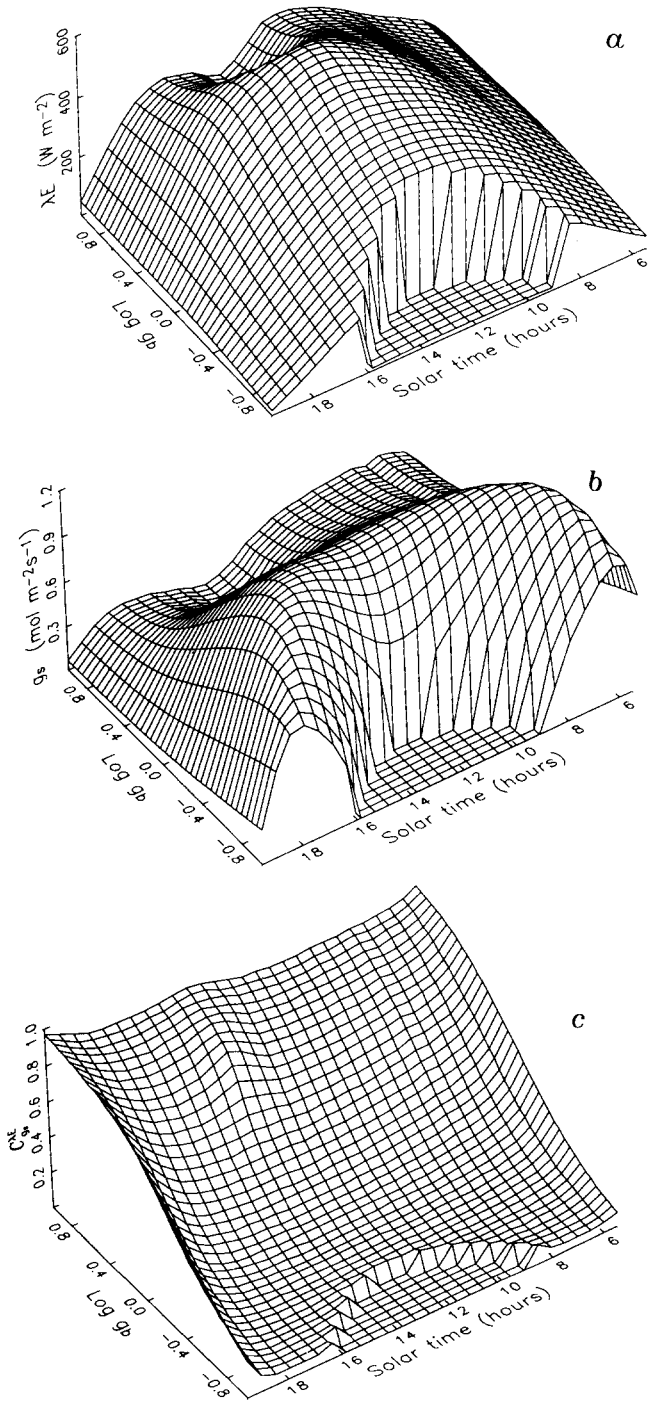
a
λE (W m⁻²)
600
400
200
0.8
0.4
0.0
-0.4
-0.8
Log gb
18
16
14
12
10
8
6
Solar time (hours)
b
gs (mol m⁻²s⁻¹)
1.2
0.9
0.6
0.3
0.8
0.4
0.0
-0.4
-0.8
Log gb
18
16
14
12
10
8
6
Solar time (hours)
c
1.0
0.8
0.6
0.4
0.2
0.8
0.4
0.0
-0.4
-0.8
Log gb
18
16
14
12
10
8
6
Solar time (hours)

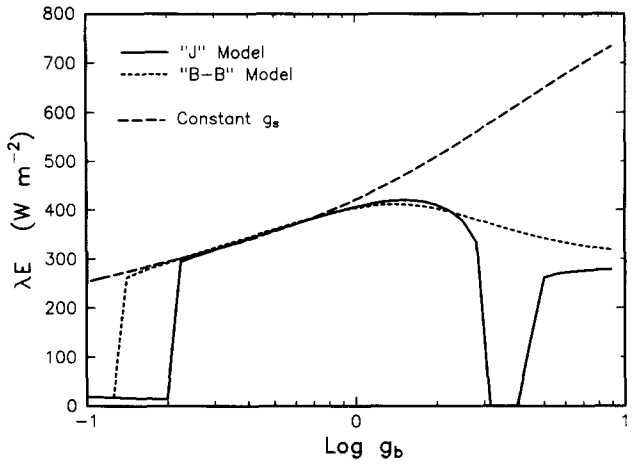

Fig. 10. Simulations of latent heat flux as a function of log boundary-layer conductance for different physiological responses. Environmental conditions are $R_s = 800$ W m^2, $e_a = 10.5$ kPa and $T_a = 25°$C. Two forms of the coupled photosynthesis, stomatal conductance model are shown, one using the Ball–Berry humidity response (B–B) (eqn. (1)) and the other using the Jarvis type humidity response (J) using eqn. (5) with g'_s as given by eqn. (8). For comparison, a plot of latent heat flux at a constant stomatal conductance (1 mol m^{-2} s^{-1}) is shown.

the responses at extreme values of g_b are useful for interpreting the feedbacks within the system.

Figure 10 shows a transect through the λE surface (Fig. 9(a)) at about 12:00 h, and compares the result with simulations obtained using altered forms of the stomatal-photosynthesis model. To assist in interpreting the response of λE to g_b, we present a three-dimensional plot of g_b (Fig. 9(b)) and a plot (Fig. 9(c)) showing the sensitivity of the modeled flux of λE to g_s ($C_{g_s}^{\lambda E} = (\partial \lambda E / \partial g_s) \times (g_s / \lambda E)$, determined by finite difference). The latter parameter is a 'control coefficient' that indicates the extent to which the output of the system is controlled by g_s at the operating point. In general, $0 < C < 1$, and a value of $C = 1$ indicates that the flux is proportional to the variable in question (i.e. it controls the flux) (see Woodrow, 1989; Woodrow et al., 1990).

Stomatal control of λE

Jarvis and McNaughton (1986) discussed the control that stomata have on λE in the context of the linearized energy balance model of Penman–Mon-

Fig. 9. (a) A three-dimensional plot of λE as a function of the time of day and the log g_b. (b) The corresponding plot of stomatal conductance. (c) A plot of the sensitivity of latent heat flux to stomatal conductance ($C_{g_s}^{\lambda E}$). Latent heat flux tends to be independent of stomatal conductance when $C_{g_s}^{\lambda E} < 0.30$, whereas higher values indicate regions of strong stomatal control of latent heat flux. The values of $C_{g_s}^{\lambda E}$ are truncated to 0 at low values of g_b where T_l reaches lethal values.

teith in which g_s and g_b are independent variables, and they define a parameter Ω ($\Omega = 1 - (d\lambda E/dg_s) \times (g_s/\lambda E)$) that indicates the extent to which λE approaches the limit of 'equilibrium evaporation'. It should be noted that Ω is similar to $1 - C_{g_s}^{\lambda E}$, as used here, with the exception that g_s is a dependent variable in our analysis. The consequence of permitting g_s to vary as predicted by the complete model is that 'Ω' (which is primarily a function of the ratio g_s/g_b) is also dependent on the regulatory responses that affect the value of g_s. Referring to Fig. 9(c), we can see that 'Ω' (1 – the plotted value) varies over the course of a day. $C_{g_s}^{\lambda E}$ tends to be larger in the morning and evening (stomata are more in control) than at midday, and $C_{g_s}^{\lambda E}$ increases under conditions where midday stomatal closure occurs. $C_{g_s}^{\lambda E}$ becomes larger (stomata exert more control) as the boundary-layer conductance increases, and it increases again as $g_b \to 0.1$ mol m^{-2} s^{-1} where $g_s \to 0$ (when $g_s = 0$, $C_{g_s}^{\lambda E}$ is undefined and truncated to 0 in Fig. 9(c)). At $g_b < 1$ mol m^{-2} s^{-1}, $C_{g_s}^{\lambda E}$ is generally small, indicating (as proposed by Jarvis and McNaughton (1986)) that stomata exert little control over λE when g_b is low. Nevertheless, very substantial changes in g_s occur over this range of g_b (see Fig. 9(b)). It may be unwise to dismiss these stomatal responses as having no significance. We note that the opening of stomata when g_b is low tends to decrease T_l and increase p_i, both of which may have substantial effects on photosynthesis. This is an area which needs further attention.

Discussion of midday responses

For the purpose of discussion, and referring to Figs. (7), (9) and (10), we can distinguish three different types of midday response.

(1) In the intermediate range of g_b (0.2–1 mol m^{-2} s^{-1}), λE appears to track the input of R_s and increases as g_b increases (Figs. 9(a) and (10)). This is opposite to the response of g_s which tends to decrease while λE increases (compare Fig. 9(a) and 9(b)). This corresponds to a region where $C_{g_s}^{\lambda E} < 0.4$ (Fig. 9(c)), indicating that the flux is relatively insensitive to g_s. Figure 10 shows that λE over this range of g_b is insensitive to the form of the sub-model used to specify g_s. For example, assuming that $g_s = 1$ mol m^{-2} s^{-1} yields nearly identical λE over this range of g_b. In this region, the λE approaches that of a wet surface. Some feedback regulation of g_s occurs as a result of temperature and humidity interactions (Fig. 9(b)), but the physiological system does not become unstable, and T_l and g_s co-vary so that λE tracks R_s.

(2) At low g_b (< 0.2 mol m^{-2} s^{-1}), there is precipitous closure of stomata during midday (Figs. 9(b) and 10)). Examination of model output (data not shown) reveals that leaf temperatures rise beyond levels known to cause permanent damage to the photosynthetic reactions of leaves. The total collapse of the physiological component in this region of g_b is apparently driven by the tendency for heat to be trapped within the boundary layer at low values

of g_b, as sensible and latent heat fluxes are restricted. Consequently, leaf temperature increases as g_b decreases and when T_l exceeds the temperature optimum for photosynthesis, A_n and g_s begin to fall. This response is accelerated by positive feedback mediated by a decrease in h_s and increase in T_l as g_s is decreased. Eventually, the physiological system becomes unstable with T_l approaching 70°C. Similar feedbacks affecting T_l have been observed in the laboratory and in the field as T_l approaches the lethal limit (Gamon and Pearcy, 1989). In the real world, there would be strong selective pressure against leaf properties that would lead to such high values of T_l. In Fig. 10, we show that the abrupt stomatal closure occurs at higher g_b (e.g. stronger feedbacks) if we introduce the humidity response of the J model (eqn. (5)) which does not include changes in the response to $\mathscr{D}_s$ with changes in T_l.

(3) At values of g_b exceeding about 2 mol m^{-2} s^{-1}, a midday depression in λE begins to appear (Figs. 9(a) and (10)). This is associated with a decline in g_s (Fig. 9(b)) and an increase in the sensitivity coefficient for λE as a function of g_s (Fig. 9(c)). This depression in λE flux is not seen when the humidity response components are eliminated from the model, but it becomes more pronounced when the $\mathscr{D}_s$ response (J model) is substituted for the h_s (Fig. 10). Thus, this response is related to the regulation of h_s by atmospheric humidity. $\mathscr{D}_a$ and T_l peak near 14:00 h (Fig. 6) and h_s should tend to reach a minimum at this time. The value of h_s should decrease as g_b increases, eventually approaching the humidity of the ambient air. The model includes an additional feedback arising from the decrease in A_n (see Fig. 7(c)) and p_i falls. The existence of positive feedback loops tends to make the system unstable with respect to changes in g_s (i.e. a perturbation that would cause g_s to increase or decrease can elicit other changes in the system which tend to amplify the response). In this regard, it is interesting to note that a characteristic of the B–B model tends to add stability to the system. This can be seen by comparing the responses at extreme values of g_b with either the J model or the B–B model (see Fig. 10). When compared with a simple response to $\mathscr{D}$, the temperature-compensated response of the B–B model (see Fig. 5) tends to decrease positive feedback (involving humidity), leading to stomatal closure, and tends to increase that leading to opening of stomata.

Effects of physiological capacity and CO_2 concentration

The capacity of physiological components of this system and the value of c_a also influence the response properties, as illustrated in Fig. 11. For example, a simulation where V_m was reduced by 33% is shown in Fig. 11(b). The control, Fig. 11(a), is identical to Fig. 9(a). λE is not affected when Q_p is low in the morning and evening, but is lower during midday. The depressions in λE at high and low g_b, seen in Figs. 7 and 9(a), are expanded. With further reduction in V_m (not shown), the two depressions merge so that stomata al-

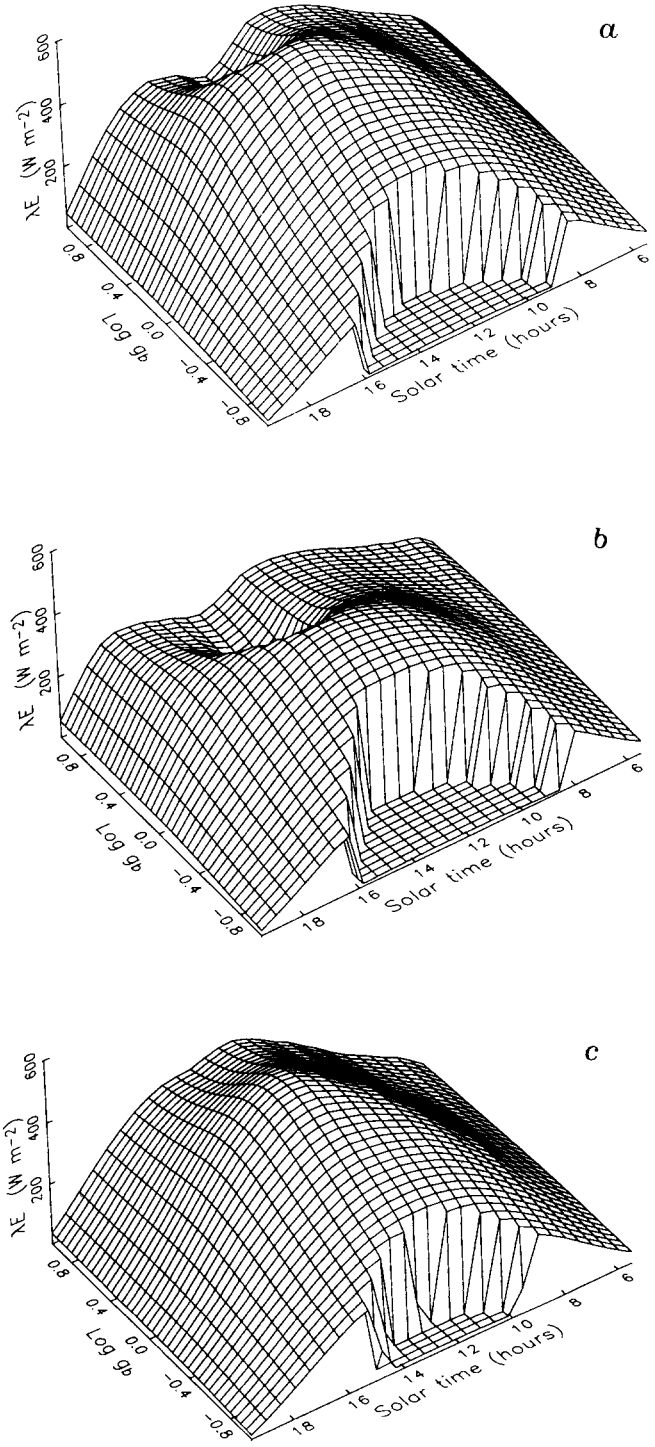
a
b
c
λE (W m-2)
200
400
600
Log gb
0.8
0.4
0.0
-0.4
-0.8
Solar time (hours)
6
8
10
12
14
16
18

ways close in high R_s, regardless of the value of g_b. The effect can be reversed by lowering R_s or increasing the value of m. Plants with low photosynthetic capacity should, therefore, not occur in high-radiation environments or, if they do, they should not have large leaves. Forest understory leaves are typically large and have low photosynthetic capacities, but of course they operate in environments characterized by low radiation and low $\mathscr{D}$. V_m may change according to environmental and physiological conditions on time scales from weeks to years in response to average light intensity (Wong et al., 1985a), soil nitrogen (Wong et al., 1985a) and water stress (Wong et al., 1985c). The simulations shown here indicate that changes in the physiological properties of the leaves making up a canopy may affect the exchange of λE.

The CO_2 concentration of the atmosphere has risen approximately by 70 ppm this century and the CO_2 concentration may double over present levels in the next century. It is of some interest, therefore, to examine how higher CO_2 concentrations might affect the energy exchange of plant canopies. Figure 11(c) shows a simulation with c_a twice the present level (all else identical to Fig. 11(a)). The simulation shows that increased CO_2 causes a small decrease in λE at intermediate values of g_b and it tends to result in increased λE at the extremes of g_b (where midday depressions occur in normal c_a). This effect is not intuitively obvious. Consider eqn. (1), increasing c_s should cause g_s to decrease, but in the complete model g_s is in fact increased by increased CO_2, at least over some ranges of g_b. This occurs because increasing CO_2 tends to eliminate the positive feedback loop in g_s that is mediated by effects on p_i and A_n. At higher CO_2, A_n is higher and is less sensitive to changes in p_i. It will be interesting to see if this occurs in real systems.

CONCLUSIONS

The system of models developed here permits simulation of the transpiration and energy balance of a simple canopy using physiologically driven submodels for photosynthesis and regulation of stomatal conductance. The predictive capacity of the physiological sub-models was examined in extensive gas exchange studies with attached intact leaves of soybean, and the tests show the model can be applied to a wide range of environmental conditions. The physiological models were included in a leaf energy balance and mass transport model structured to permit stomatal responses to be driven by the conditions in the local region of the stomata (i.e. at the leaf surface) through a boundary layer of air adjacent to the leaf. Simulations indicate that the con-

Fig. 11. Three-dimensional plots showing the effect of changing the V_m Rubisco and the concentration of CO_2 on the flux of latent heat flux as a function of time of day and log boundary-layer conductance. (a) Control, identical to Fig. 9(a). (b) An identical simulation with $V_m = 0.67$ times the control value. (c) An identical simulation with c_a twice the control value.

ductance of a leaf boundary layer can have significant influences on the canopy response properties. For example, simulation of a day curve (using the same ambient conditions and physiological properties) assuming different values of g_b, results in very different patterns. With a low g_b, λE is nearly proportional to R_s over the entire day, while with $g_b = 8$ mol m^{-2} s^{-1}, a strong midday depression of λE is observed. Further examination of the response to g_b shows that midday stomatal closure can be driven by excessively high leaf temperature (at low values of g_b) and by drying of the air at the leaf surface (at high values of g_b). These responses interact with the photosynthetic capacity of the leaf (which affects g_{max}), with the radiation load on the canopy, and with the CO_2 concentration of the air. Similar response patterns are known to occur with natural vegetation of different types. The models presented here provide a plausible mechanism for these responses. Experimental studies at the canopy level are required to test the mechanisms proposed here.

ACKNOWLEDGEMENTS

The authors would like to thank Drs. Toby Carlson, Chris Field and Ian Woodrow for helpful suggestions in the preparation of the manuscript. Drs. Ray Leuning and Keith Mott provided preprints of their manuscripts. This paper was written as a direct result of a workshop on stomatal resistance held at Pennsylvania State University, 10–13 April 1989. The workshop was made possible principally through a grant from the National Science Foundation (BSR-8822164).

REFERENCES

Avissar, R., Avissar, P., Mahrer, Y. and Bravdo, B.A., 1985. A model to simulate response of plant stomata to environmental conditions. Agric. For. Meteorol., 34: 21–29.

Ball, J.T., 1987. Calculations related to gas exchange. In: E. Zeiger, G.D. Farquhar and I.R. Cowan (Editors), Stomatal Function. Stanford University Press, Stanford, CA, pp. 446–476.

Ball, J.T., 1988. An analysis of stomatal conductance. Ph.D. Thesis, Stanford University, CA, 89 pp.

Ball, J.T. and Berry, J.A., 1982. The c_i/c_s ratio: A basis for predicting stomatal control of photosynthesis. Carnegie Institute Washington Yearbook, 81: 88–92.

Ball, J.T. and Berry, J.A., 1991. An analysis and concise description of stomatal responses to multiple environmental factors. Planta, in press.

Berry, J.A. and Raison, J.K., 1981. Responses of macrophytes to temperature. In: O.L. Lange, P.S. Nobel, C.B. Osmond and H. Ziegler (Editors), Encyclopedia of Plant Physiology, 12A. Springer-Verlag, Berlin, pp. 277–338.

Beyschlag, W., Lange, O.L. and Tenhunen, J.D., 1986. Photosynthesis and water relations of the mediterranean evergreen sclerophyll *Arbutus unedo* L. through out the year at a site in Portugal. I. Diurnal courses of CO_2 gas exchange and transpiration under natural conditions. Flora, 178: 178–444.

Björkman, O., Badger, M.R. and Armond, P.A., 1980. Response and Adaptation of Photosynthesis to High Temperatures. Wiley-Interscience, New York, pp. 233–349.

Brooks, A. and Farquhar, G.D., 1985. Effects of temperature on the CO_2/O_2 specificity of ribulose-1,5 bisphosphate carboxylase/oxygenase and the rate of respiration in the light. Planta, 165: 397–406.

Cambell, D.I., 1989. Energy balance and transpiration from a tussock grassland in New Zealand. Boundary-Layer Meteorol., 46: 133–152.

Choudhury, B.J. and Monteith, J.L., 1986. Implications of stomatal response to saturation deficit for the heat balance of vegetation. Agric. For. Meteorol., 35: 153–164.

Collatz, G.J., Berry, J.A., Farquhar, G.D. and Pierce, J., 1990. The relationship between the rubisco reaction mechanism and models of photosynthesis. Plant Cell Environ., 13: 219–225.

Cowan, I.R., 1977. Stomatal behavior and environment. Adv. Bot. Res., 4: 117–228.

Cowan, I.R. and Farquhar, G.D., 1977. Stomatal function in relation to leaf metabolism and environment. Symp. Soc. Exp. Biol., 31: 471–505.

Evans, J.R. and Seemann, J.R., 1989. The allocation of protein nitrogen in the photosynthetic apparatus: costs, consequences and control. In: W.R. Briggs (Editor), Photosynthesis. Liss, New York, pp. 182–205.

Farquhar, G.D., 1978. Feedforward response of stomata to humidity. Aust. J. Plant Physiol., 5: 787–800.

Farquhar, G.D. and Sharkey, T.D., 1982. Stomatal conductance and photosynthesis. Annu. Rev. Plant Physiol., 33: 317–45.

Farquhar, G.D., von Caemmerer, S. and Berry, J.A., 1980. A biochemical model of photosynthetic CO_2 assimilation in leaves of C_3 plants. Planta, 149: 78–90.

Faver, K.L. and O'Toole, J.C., 1989. Short term estimation of sorghum evapotranspiration from canopy temperature. Agric. For. Meteorol., 48: 175–183.

Gamon, J.A. and Pearcy, R.W., 1989. Leaf movement, stress avoidance and photosynthesis in *Vitus californicus*. Oecologia (Berlin), 79: 475–481.

Gash, J.H.C., Shuttleworth, W.J., Lloyd, C.R., Andre, J-C. and Goutorbe, J-P., 1989. Micrometeorological measurements in Les Landes forest during HAPEX-MOBILHY. Agric. For. Meteorol., 46: 131–147.

Grace, J., 1983. Plant–Atmosphere Relationships. Chapmann-Hall, London, 92 pp.

Idso, S.B., 1987. An apparent discrepancy between porometry and infared thermometry relative to the dependence of plant stomatal conductance to air vapor pressure deficit. Agric. For. Meteorol., 40: 105–106.

Idso, S.B., Jackson, R.D., Pinter, P.J., Reginato, R.J. and Hatfield, J.L., 1981. Normalizing the stress-degree-day parameter for environmental variability. Agric. Meteorol., 24: 45–55.

Jarvis, P.G., 1976. The interpretations of the variation in leaf water potential and stomatal conductance found in canopies in the field. Philos. Trans. R. Soc. London. Ser. B, 273: 593–610.

Jarvis, P.G. and McNaughton, K.G., 1986. Stomatal control of transpiration: scaling up from leaf to region. Adv. Ecol. Res., 15: 1–49.

Jones, H.G. and Higgs, K.H., 1989. Empirical models of the conductance of leaves in apple orchards. Plant Cell Environ., 12: 301–308.

Jordan, D.B. and Ogren, W.L., 1981. A sensitive assay procedure for simultaneous determination of ribulose-1,5-bisphosphate carboxylase and oxygenase activities. Plant Physiol., 76: 237–245.

Kirchbaum, M.V.F. and Farquhar, G.D., 1984. Temperature dependence of whole-leaf photosynthesis in *Eucalyptus pauciflora*. Sieb. ex Spreng. Aust. J. Plant Physiol., 11: 519–538.

Lindroth, A. and Halldin, S., 1986. Numerical analysis of pine forest evaporation and surface resistance. Agric. For. Meteorol., 38: 59–79.

Leuning, R., 1990. Modelling stomatal behavior and photosynthesis of *Eucalyptus grandis*. Aust. J. Plant Physiol., 17: 159–175.

MacRobbie, E.A.C., 1987. Ionic relations of guard cells. In: E. Zeiger, G.D. Farquhar and I.R. Cowan (Editors), Stomatal Function. Stanford University Press, Stanford, CA, pp. 125–162.

Mott, K.A. and Parkhurst, D.F., 1991. Stomatal responses to humidity in air and Helox. Plant Cell Environ., in press.

Norman, J.M. and Polley, W., 1989. Canopy photosynthesis. In: W.R. Briggs (Editor), Photosynthesis. Liss, New York, pp. 227–241.

O'Toole, J.C. and Real, J.G., 1986. Estimation of aerodynamic and crop resistance from canopy temperature. Agron. J., 78: 305–310.

Paw U, K.T., 1987. Mathematical analysis of the operative temperature and energy budget. J. Therm. Biol., 12: 227–233.

Raschke, K., 1979. Movements of stomata. In: W. Haupt and M.E. Feinlieb (Editor), Encyclopedia of Plant Physiology, New Series, Vol. 7, Physiology of Movement. Springer-Verlag, Berlin, pp. 383–441.

Raupach, M.R. and Finnigan, J.J., 1989. 'Single-layer models of evaporation from plant canopies are incorrect but useful whereas multilayer models are correct but useless': Discuss. Aust. J. Plant Physiol., 15: 705–716.

Sato, N., Sellers, P.J., Randall, D.A., Schneider, E.K., Shukla, J., Kinter III, J.L., Hou, Y-T. and Albertanzi, E., 1989. Effects of implementing the simple biosphere model in a global circulation model. J. Atmos. Sci., 46: 2757–2782.

Stewart, J.B., 1988. Modelling surface conductance of pine forests. Agric. For. Meteorol., 43: 19–35.

Tan, C.S. and Black, T.A., 1976. Factors affecting the canopy resistance of a Douglas-Fir Forest. Boundary-Layer Meteorol., 10: 475–488.

Weis, E. and Berry, J.A., 1988. Plants and high temperature stress. In: S.P. Long and F.I. Woodward (Editors), Plants and Temperature. Soc. Exp. Biol., 42: 329–346.

Wong, S.C., Cowan, I.R. and Farquhar, G.D., 1978. Leaf conductance in relation to assimilation in *Eucalyptus pauciflora* Sieb. ex Spieng: Influence of irradiance and partial pressure of carbon dioxide. Plant Physiol., 62: 670–674.

Wong, S.C., Cowan, I.R. and Farquhar, G.D., 1979. Stomatal conductance correlates with photosynthetic capacity. Nature, 282: 424–426.

Wong, S.C., Cowan, I.R. and Farquhar, G.D., 1985a. Leaf conductance in relation to rate of CO_2 assimilation. I. Influence of nitrogen nutrition, phosphorous nutrition, photon flux density and ambient partial pressure of CO_2 during ontogeny. Plant Physiol., 78: 821–825.

Wong, S.C., Cowan, I.R. and Farquhar, G.D., 1985b. Leaf conductance in relation to rate of CO_2 assimilation. II. Effects of short term exposure to different photon flux densities. Plant Physiol., 78: 826–829.

Wong, S.C., Cowan, I.R. and Farquhar, G.D., 1985c. Leaf conductance in relation to rate of CO_2 assimilation. III. Influence of water stress and photoinhibition. Plant Physiol., 78: 830–834.

Woodrow, I.E., 1989. Limitation to CO_2 fixation by photosynthetic processes. In: W.R. Briggs (Editor), Photosynthesis. Liss, New York, pp. 457–501.

Woodrow, I.E. and Berry, J.A., 1988. Enzymatic regulation of photosynthetic CO_2 fixation in C_3 plants. Annu. Rev. Plant Physiol., 39: 533–594.

Woodrow, I.E., Ball, J.T. and Berry, J.A., 1990. Control of photosynthetic carbon dioxide fixation by the boundary layer, stomata and ribulose-1,5-bisphosphate carboxylase/oxygenase. Plant Cell Environ., 13: 339–347.

APPENDIX

Photosynthesis model

Leaf photosynthesis is described here as the minimum of three potential capacities or

$$\boldsymbol{A} \approx \min \begin{cases} J_E \\ J_C \\ J_S \end{cases} \tag{A1}$$

where $\boldsymbol{A}$ is the rate of gross CO_2 uptake, and J_E and J_C are defined according to Farquhar et al. (1980).

J_E describes the response of photosynthetic to $\boldsymbol{Q}_p$ as

$$J_E = a \times \alpha \times \boldsymbol{Q}_p \frac{p_i - \Gamma_*}{p_i + 2\Gamma_*} \tag{A2}$$

where a is leaf absorptance to photosynthetically active radiation, α is the intrinsic quantum efficiency for CO_2 uptake, and Γ_* is defined by the equation

$$\Gamma_* = \frac{[O_2]}{2\tau} \tag{A3}$$

where τ is a ratio of kinetic parameters describing the partitioning of RuBP to the carboxylase or oxygenase reactions of Rubisco. τ can be determined experimentally from gas exchange experiments on intact leaves (see Brooks and Farquhar, 1985) or from enzymatic analysis in vitro (see Jordan and Ogren, 1981). $[O_2]$ is assumed constant (209 mmol mol^{-1}), p_i is given by $p_i = P \times c_i$, and

$$c_i = c_a - \boldsymbol{A}_n \frac{1.6g_s + 1.4g_b}{2.24g_s g_b} \tag{A4}$$

Note that c_a, c_i and diffusion gradients are in mole fraction, while the kinetic expressions for biochemical reactions require partial pressure, and P is the atmospheric pressure.

J_C is the Rubisco-limited rate and is defined as

$$J_C = \frac{V_m(p_i - \Gamma_*)}{p_i + K_c(1 + [O_2]/K_o)} \tag{A5}$$

where K_c and K_o are the Michaelis constant for CO_2 and the competitive inhibition constant for O_2 with respect to CO_2 in the Rubisco reaction, and V_m is the maximum catalytic capacity of Rubisco per unit leaf area (μmol m^{-2} s^{-1}). For the calculations presented in Figs. 3 and 4, V_m was determined from measurements of the slope of the response of $\boldsymbol{A}_n$ to p_i at $p_i = \Gamma_*$, according to

$$V_m = \frac{dA_n}{dp_i}\left[\Gamma_* + K_c\left(1 + \frac{[O_2]}{K_o}\right)\right] \quad (A6)$$

(see Collatz et al., 1990).

J_S is the capacity for the export or utilization of the products of photosynthesis (most likely sucrose synthesis, see Woodrow and Berry, 1988), and this is approximately the maximum value of A_n at saturating Q_p and CO_2. Here, we use

$$J_S = V_m/2 \quad (A7)$$

Equation (A1) is equivalent in form to that proposed by Kirchbaum and Farquhar (1984), but our definitions of J_C, J_E and J_S differ somewhat from theirs.

To introduce a more realistic, gradual transition from one limitation to another, and to allow for some co-limitation between J_E, J_C and J_S, we solve the following two quadratics for their smaller roots.

$$\theta J_P^2 - J_P(J_E + J_C) + J_E J_C = 0 \quad (A8)$$

and

$$\beta A^2 - A(J_P + J_S) + J_P J_S = 0 \quad (A9)$$

where A is the gross rate of CO_2 uptake, and J_P is an intermediate variable that gives the minimum of J_E and J_C. θ and β are empirical constants describing the transition between limitations, and are typically close to one (here we use 0.98 and 0.95, respectively).

Respiratory CO_2 production (R_d) was scaled to the V_m as

$$R_d = 0.015 V_m \quad (A10)$$

(see Farquhar et al., 1980) and A_n is then defined as

$$A_n = A - R_d \quad (A11)$$

Some of the kinetic parameters of the model, K_c, τ, K_o, V_m (and the fluxes R_d and J_S), change with temperature. We used the Q_{10} function

$$k = k_{25} Q_{10}^{(T_l - 25)/10} \quad (A12)$$

where k_{25} is the parameter value at 25 °C and Q_{10} is the relative change in the parameter for a 10 °C change in temperature. Values for the parameters and respective Q_{10} are given in Table A1 (see also Woodrow and Berry, 1988).

The combined temperature response of A_n described above does not account for the well-known thermal inhibition at temperatures exceeding 35 °C (Berry and Raison, 1981). In order to simulate realistic rates at high temperature, we introduced to the model a gradual temperature inhibition of the V_m described by

$$V_m = V_m^o \left\{ 1 + \exp\left[\frac{-a + b(T_l + 273)}{R(T_l + 273)} \right] \right\}^{-1} \quad \text{(A13)}$$

where the superscript o indicates an intermediate value, corrected according to eqn. (A12) to T_l (see Weis and Berry, 1988). R is the ideal gas constant, and a and b are constants.

R_d is also inhibited at high temperature and for this response we use the following form

$$R_d = R_d^o \{ 1 + \exp[1.3(T_l - 55)] \}^{-1}$$

which predicts an abrupt collapse in R_d as T_l approaches 55 °C (see Björkman et al., 1980).

TABLE A1

Values of kinetic parameters and constants used in the models of stomatal conductance, photosynthesis and energy balance[1]

Symbol	Value	Units	Q_{10}	Description
a	220	KJ mol^{-1}		(Equation (A13))
a	0.86			Leaf absorptance to Q_p (eqn. A2))
b	703	J/mol °K		(Equation (A13))
b	0.01	mol m^{-2} s^{-1}		Intercept, B–B model (eqn. (1))
c_a	340	μmol mol^{-1}		Ambient mole fraction CO_2
J_S	100	μmol m^{-2} s^{-1}	2.4	Sink capacity (eqn. (A7))
K_c	30	Pa	2.1	Michael is constant, CO_2 (eqn. (A5))
K_o	30	kPa	1.2	Inhibition constant of O_2 (eqn. (A5))
m	9			Slope parameter, B–B model (eqn. (1))
m'	31			Slope parameter, J model
m''	167			Slope parameter, L model
O_2	20.9	kPa		Partial pressure O_2
P	10^5	Pa		Atmospheric pressure
R_d	3	μmol m^{-2} s^{-1}	2.0	'Day' respiration (eqn. (A10))
R_{sky}	340	W m^{-2}		Long wave-length radiation from sky
V_m	200	μmol m^{-2} s^{-1}	2.4	Rubisco capacity (eqn. (A5))
α	0.08			Quantum efficiency (eqn. (A2))
β	0.98			(Equation (A9))
τ	2600		0.57	CO_2/O_2-specificity ratio (eqn. (A3))
θ	0.95			(Equation (A8))

[1]Symbols for variables used in the models. A, gross CO_2 assimilation; A_n, net CO_2 assimilation; c, CO_2 mole fraction (subscripts refer to the ambient air, a, leaf surface, s, and intercellular air spaces, i, and are used uniformly for all other variables); p, CO_2 partial pressure; C, a control coefficient; $\mathscr{D}$, the vapor pressure gradient (water); e, the partial pressure of water vapor; e^*, the saturation vapor pressure of water at a specified temperature; h_s, relative humidity at the leaf surface; g_b, boundary-layer conductance; g_s, stomatal conductance; g_{max}, maximum stomatal conductance; J_C, the 'Rubisco-limited' capacity for CO_2 fixation; J_E, the 'Q_p-limited' capacity for A_n; J_S, the 'sink-limited' capacity for A_n; Γ_*, the p_i at which $A=0$; λE, the flux of latent heat carried by transpired water vapor; Q_p, the incident flux of photosynthetically active photons; R_s, the solar radiation; R_t, the total radiation; T_a, the temperature of the ambient air; T_l, the leaf temperature; RuBP, ribulose 1,5-bisphosphate.

Energy balance sub-model

Surface temperature is calculated from the explicit solution of a fourth-order approximation to the energy budget equation given by Paw U (1987). The response of e^* to temperature is described by a fourth-degree regression approximation of the Goff–Gratch equation, and regression constants are given by Paw U (1987). λE and sensible heat flux are calculated from surface temperature and g_s using the usual molecular flux equations. The surface is considered to be horizontal, uniform and single sided. Vertical gradients through the surface in R_s, humidity, temperature and g_b are not considered.